AD-A160 145 SURFACE INFRARED REFLECTION-ABSORPTION SPECTROSCOPY USING A TUNABLE DIODE LASER(U) NAVAL RESEARCH LAB WASHINGTON DC J E BUTLER ET AL. 01 OCT 85 TR-1 1/1

UNCLASSIFIED F/G 7/4 NL

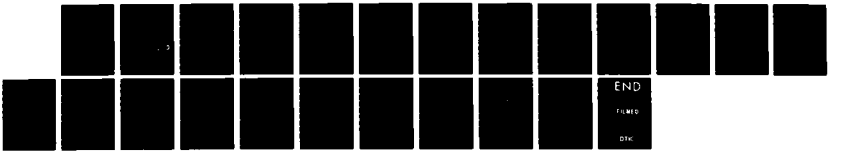

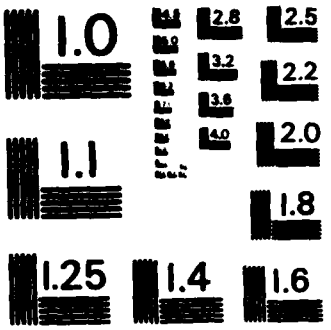

MICROCOPY RESOLUTION TEST CHART
NATIONAL BUREAU OF STANDARDS-1963-A

OFFICE OF NAVAL RESEARCH

Contract N00014-85-WR-24260

Task No. NR 629-851

TECHNICAL REPORT NO. 1

Surface Infrared Reflection-Absorption Spectroscopy Using A Tunable Diode Laser

by

James E. Butler, Victor M. Bermudez, and Jeff L. Hylden

Prepared for Publication

in the

Journal of Surface Science

Naval Research Laboratory
Washington, D.C. 20375-5000

October 1, 1985

SURFACE INFRARED REFLECTION-ABSORPTION SPECTROSCOPY USING A TUNABLE DIODE LASER

J.E. BUTLER, V.M. BERMUDEZ AND J.L. HYLDEN*
NAVAL RESEARCH LABORATORY
WASHINGTON, D.C. 20375-5000
U.S.A.

ABSTRACT

Single-reflection infrared reflection-absorption spectra (IRRAS) of adsorbates on surfaces have been obtained using a tunable diode laser radiation source. Surface sensitivity is achieved through the use of polarization modulation, and the high brightness of the laser light source has made possible the observation of vibrational modes at energies much lower than those accessible with conventional blackbody sources. Results are presented for the chemisorption of oxygen on polycrystalline aluminum showing surface (580/cm^{-1}) and subsurface (890/cm^{-1}) Al-O stretching modes at sub-monolayer coverage.

*NRC/NRL Resident Research Associate

INTRODUCTION

Much of the effort in contemporary surface science is directed toward the identification of the chemical environment in the vicinity of an adsorbate atom or molecule. Information of this sort is profoundly important in studies of catalysis, surface reactions, thin-film growth and interface properties. The electron spectroscopic approaches familiar to UHV/surface science - Auger, photoemission, electron energy-loss and low-energy electron diffraction - have made significant impact on these problems in the past fifteen years. However, in many cases, specific chemical information is provided only indirectly and not without the need for quantitative theoretical analysis.

Vibrational spectroscopy has the potential for supplying a more direct

and unambiguous identification of chemical bonding through measurement of the characteristic frequencies of surface functional groups. To date, high-resolution (~5 meV = 40 cm^{-1}) electron energy-loss spectroscopy (EELS) has been the most widely used technique for vibrational studies at sub-monolayer coverages [1,2]. EELS is fairly easy to implement and permits rapid coverage of the entire vibrational energy range (200 to 4000 cm^{-1}). However, a reasonably high vacuum ($<10^{-5}$ torr) is required during measurement which precludes any form of real-time or in-situ study of surface reactions under so-called "practical" conditions. Second, electron impact and/or the presence of a hot-filament electron source can, in some cases, significantly alter the surface chemistry under investigation [3,4]. Finally, EELS resolution is, at present, limited to about 40 cm^{-1}. Hence, lineshapes and peak positions cannot be precisely determined.

In principle, optical spectroscopy can circumvent all of these problems by providing a high-resolution and non-invasive probe usable in any transparent ambient. In practice infrared spectroscopy at sub-monolayer coverage has been severely restricted by the limited intensity available from conventional blackbody radiation sources [5]. Several methods have been developed to deal with this problem. For example, one can increase the effective surface area through the use of supported powders [6] or multiple reflections [7]. However, this places certain constraints on the nature of the sample and surface preparation. Infrared emission spectroscopy [8] has recently been applied to adsorbates, but a cryogenically cooled monochromator and collection optics are required at wavelengths beyond a few microns. Synchrotrons appear promising [5,9] as sources at wavelengths as long as 100μ; however, access to such facilities is not readily available to the general user.

The long-range goal of the work reported here is the development of a generally applicable technique for surface infrared reflection absorption spectroscopy (IRRAS) providing high resolution (10 cm^{-1} or better) at energies down to 350 cm^{-1} for the purpose of studying surface chemical reactions under "practical" conditions. The program is founded on the use of tunable solid-state diode lasers as brighter sources of IR radiation. Other than the work of Lambert [10] on the electroreflectance spectrum of CO on Ni, this is the first use of diode lasers in IRRAS.

DESIGN CONSIDERATIONS

The essential problem in single-reflection IRRAS is the detection of very weak adsorbate-induced structure in the presence of a much stronger (by three orders of magnitude or more) background arising from the substrate. To date, two approaches have been developed [9]. The first takes advantage of the fact that the adsorbate linewidth is narrow in contrast to the background. Hence, recording the derivative [9,11,12] of the reflectance with respect to wavelength can enhance the adsorbate-induced structure. While this method has been applied successfully in a number of UHV studies, it does not discriminate between absorptions in the ambient and in the adsorbate layer. The same difficulty occurs in double-beam techniques [9,13].

The second approach involves polarization modulation [9,14-19] in which the difference in reflected intensity polarized parallel (p) and perpendicular (s) to the plane of incidence is recorded. For a grazing angle of incidence (80^{o} or more) on a metal surface [9], the p-polarized electric field intensity is much larger than at smaller angles and is several orders of magnitude greater than that for s-polarization. Hence, only p-polarized light can couple to adsorbate vibrations, and only modes normal to the surface can be excited. When the modulated signal is normalized to the total reflected

intensity, polarization modulation IRRAS effectively discriminates against absorption by species in the isotropic gaseous ambient. A distinct advantage of the diode laser in this application is that the narrow well-collimated beam permits precise control of the angle of incidence.

Polarization modulation may be implemented by placing a mechanically rotating polarizer [14-17] immediately before or after the sample. In one approach [14,15], the rotator-sample pair is positioned between two fixed polarizers. In this case, the detected waveform consists of signals at the second and fourth harmonic of the rotation frequency. The phase shifts of the two components relative to the polarizer rotation are measured, from which the absorption spectrum is obtained. This method can be advantageous when the signal intensity is low [14]. A second approach [16,17] places the sample between a single fixed polarizer and the rotator and uses lock-in amplification for signal processing. We have used a variation of the latter method, described below. Since IR polarizers can be fabricated [20] by depositing wire grids on any transparent substrate, the rotating polarizer approach is suitable in the long-wavelength IR.

In an obvious alternative technique [18,19], the rotating polarizer is replaced by the combination of a fixed polarizer and a piezobirefringent (photoelastic) modulator. Over the wavelength range for which it is useable ($\lambda < 15\mu$), the photoelastic modulator (PEM) [21,22] offers the advantages of very high modulation frequency (> 50 kHz), freedom from interfering signals and the absence of moving parts.

EXPERIMENTAL ARRANGEMENT

Fig. 1 shows a schematic of the optical and electronic arrangement. Figs. 2 and 3 show the emission characteristics of diodes available in the

present apparatus. The lead salt tunable diode lasers are predominantly of the "mesa-stripe" design (Spectra-Physics/Laser Analytics Division). The bandgap of individual diodes can be temperature tuned by as much as 325 cm^{-1} (Fig. 2), and at a given temperature lasing occurs on multiple modes spanning 3 to 40 cm^{-1} (Fig. 3). When filtered by a mode-sorting monochromator, resolution of the order of 0.0003 cm^{-1} can be achieved. In these experiments, the monochromator is not used, so that the resolution (typically 30-40 cm^{-1}) is limited by the particular characteristics of each diode. Scans are performed by heating a diode to near its maximum operating temperature, turning off the heater and allowing the refrigerator to cool the cold head on which the diodes were mounted. Scans from 90°K to 15°K require 10 minutes and usually cover 250 to 300 cm^{-1}. With four diodes mounted in the cold head, a range of about 1000 cm^{-1} can be achieved. Typically, the emission in each mode is strongly polarized in the vertical direction (parallel to the current flow). In order to make the multi-mode emission emulate a continuum, the diode temperature is modulated by applying a small AC current (about 15 kHz) which has the effect of "smearing out" the mode structure in the output. The effects of residual mode structure are reduced by the intensity stabilization techniques discussed below.

The light emerging from the diode is chopped, to provide discrimination against blackbody radiation from optical components after the chopper, and passed through a vertically-oriented polarizer. The attenuation of the beam is then adjusted dynamically during a scan by the servo-controlled polarizer so as to provide intensity normalization (see below). The light is then passed through another polarizer with an azimuth set to provide nearly equal s- and p-polarized reflected intensity, thus increasing the dynamic range (sensitivity to small changes in $I_s - I_p$). In the following discussion, I_s and

I_p will refer to the detected signals corresponding to s- and p-polarized reflectance, respectively. After reflection from the sample at grazing incidence ($\theta \approx 87^o$) the light passes through the rotating polarizer and is focused by a KBr lens onto a liquid nitrogen cooled HgCdTe detector.

The detector signal is amplified, band-pass filtered and sent to a voltage-controlled amplifier (VCA). The purpose of the VCA is to compensate for the slow response of the servo-controlled polarizer in eliminating low-frequency (a few Hz) fluctuations in the laser output and abrupt changes in power resulting from the onset of new modes. The VCA is controlled by a low-gain difference amplifier which balances a reference voltage and a voltage proportional to the normalization signal. The VCA output is then demodulated by a lock-in amplifier tuned to the chopper frequency (ω_c = 5 kHz) with a time constant set sufficiently low to pass the 250 Hz signal. As discussed below, the 250 Hz waveform is the sum of a large sin(2θ) and a small cos(2θ) term, with the latter being the quantity of interest. The lock-in output is band-pass filtered at 250 Hz and sent to two gated integrator ("boxcar") modules which are triggered 90° out of phase, with gate widths of about 15 μsec. The trigger pulses are generated by a photodiode in combination with a two-blade wheel attached to the rotating polarizer. One boxcar is triggered at θ = 0° and 180°, giving (I_s-I_p) and the other at θ = 90° and 270°, giving - (I_s-I_p). The computer combines the two outputs to obtain four readings of (I_s-I_p) each polarizer cycle giving a data rate of 500 Hz. A third boxcar provides the normalization signal controlling the VCA and the servo-driven polarizer. This unit is gated at the positive maxima of the sin(2θ) waveform which results in this quantity being held constant.

An elementary Jones-matrix treatment [23] can be used to derive the detected signal. First consider the case in which light is linearly polarized

with an azimuth angle ϕ (relative to the sample s-axis) then reflects off the sample and passes through another polarizer with azimuth angle Θ. The detected intensity (assuming a polarization-independent detector) is given by

$$I = 1/2\{r_s^2\cos^2\phi + r_p^2\sin^2\phi\} + 1/2\{r_s^2\cos^2\phi - r_p^2\sin^2\phi\}\cos(2\Theta) + 1/2\{r_s r_p \cos\Delta \sin(2\phi)\}\sin(2\Theta) \quad (1)$$

where r_p and r_s are the magnitudes of the complex amplitude reflection coefficients [23], $\tilde{r}_p = r_p\exp(i\delta_s)$ and $\tilde{r}_s = r_s\exp(i\delta_s)$, and the familiar ellipsometric angles are given by $\tan\psi = r_p/r_s$ and $\Delta = \delta_p - \delta_s$.

For $\phi = 45^o$ and the second polarizer continuously rotating ($\Theta = \omega t$), the detected signal is then

$$I = 1/4\{r_s^2 + r_p^2\} + 1/4\{r_s^2 - r_p^2\}\cos(2\omega t) + 1/2 r_s r_p \cos\Delta \sin(2\omega t) \quad (2)$$

If the DC signal, $I_o = 1/4\{r_s^2 + r_p^2\}$, is either maintained constant throughtout the scan (for example, by varying the amplifier gain) or divided into the AC intenstiy, $I_{2\omega}$, the normalized AC signal is given by

$$I_{2\omega}/I_o = a'\{\cos(2\psi)\cos(2\omega t) + \sin(2\psi)\cos\Delta\sin(2\omega t)\} \quad (3)$$

where a' is a constant dependent on the detector and amplifier gains and other characteristics of the signal processing electronics. Note that - for the double modulation technique used here - the "DC term" (I_o) is modulated at the chopper frequency and the "AC term" at both the chopper and rotating polarizer frequencies. This permits easy separation of the two quantities for the above ormalization.

Given the fact that, for a typical metal in the IR, ψ and Δ are close to 45^o and 180^o, respectively, one notes that the use of a lock-in amplifier places severe demands on the phase stability of the electronics and rotating polarizer, since the quadrature signal is at least two orders of magnitude larger than the quantity of interest (the change in $\cos(2\psi)$ induced by adsorption).

This situation has lead us to use the gated integrator ("boxcar") sampling scheme shown in Fig. (1). In this method, one boxcar is gated at Θ = 0° and 180°, giving an output proportional to $(r_s^2\cos^2\phi - r_p^2\sin^2\phi)$ and a second at Θ = 90° and 270° to give $-(r_s^2\cos^2\phi - r_p^2\sin^2\phi)$. To increase sensitivity to small absorptions, the azimuth (ϕ) of the first polarizer is adjusted to minimize the boxcar outputs for the clean surface, allowing the gains to be increased by a factor of 10 or more.

With ϕ set as described above, the detected signal is essentially a pure sine-wave, representing the $\sin(2\Theta)$ term in Eq. (1). To achieve stability, the boxcar output is normalized, not by I_o, but by the amplitude of the sine function. This is accomplished by using the output of a third boxcar, triggered at Θ = 45° and 225°, to drive both the servo-controlled polarizer and the VCA, as shown in Fig. 1, so as to maintain constant the amplitude of the sine term. The results is a normalized boxcar output of the form

$$\frac{I(\Theta = 0^o)}{I(\Theta = 45^o)} = \frac{r_s^2\cos^2\phi - r_p^2\sin^2\phi}{r_s r_p \cos\Delta \sin(2\phi)} \tag{4}$$

For a metallic substrate, for which $\delta(r_s^2)/r_s^2 \ll \delta(r_p^2)/r_p^2$, the change in the measured quantity caused by adsorption reduces to the simple form

$$\delta\left(\frac{I(\Theta = 0^o)}{I(\Theta = 45^o)}\right) = \left[\frac{r_s^2\cos^2\phi + r_p^2\sin\phi}{r_s r_p \cos\Delta \sin(2\phi)}\right]\left(\frac{\delta r_p}{r_p}\right) \tag{5}$$

where the quantity in brackets is approximately unity.

Maintaining the amplitude of the $\sin(2\Theta)$ term constant makes the measurement of adsorption-induced changes in the small $\cos(2\Theta)$ signal relatively immune to small errors in the boxcar triggering. Since the source output can vary by an order of magnitude during a scan (see Fig. 2), feedback stabilization of the normalizing signal is preferable to the simpler approach in which the computer reads the signal and divides. Proper triggering is

achieved by observing the 250 Hz signal and the pulse train as the polarizer before the sample is rotated. The computer reads the constant output of the third boxcar and normalizes the signals from the first two. The computer also monitors the diode laser temperature from which the photon energy is determined in a separate calibration experiment.

RESULTS

To demonstrate the performance of the system, we have obtained spectra of a monolayer of oxygen chemisorbed on aluminum. This particular system was selected because the vibrational spectra [24,25] exhibit complex and interesting behavior, and the normal modes are near the lower limit of the presently accessible energy range. The sample was a 2 mm thick polycrystalline plate of 99.999% purity mounted in a small UHV chamber (base pressue $< 4 \times 10^{-10}$ torr) equipped with a quadrupole mass spectrometer, a Kelvin probe, an ion gun and KBr IR windows. The sample was etched in 50% aqueous HF before mounting, then cleaned by argon-ion bombardment at 3 keV for several hours. The cleanliness of the surface was verified by the observation of an immediate decrease in work function ($\delta\Phi$) when high-purity O_2 was admitted to the chamber with continuous pumping. $\delta\Phi$ was observed to saturate at about -200 meV within the first 100 L [1 L (Langmuir) = 10^{-6} torr-sec]. Upon evacuation of the O_2, $\delta\Phi$ was found to be partially reversible, turning in the positive direction. This behavior has been observed and interpreted previously [26] for the Al (111) surface. The O_2 exposures used in this study were 300 L or less, and pressures were measured with a cold-cathode ionization gauge to avoid generating excited oxygen species [4]. Since ellipsometric and work function data [26] suggest that the surface coverage changes very slowly within several hundred Langmuirs after the first 100 L, we assume that the oxygen coverage was, at most, a monolayer.

The spectra obtained, shown in Figs. 4 and 5, reveal bands at 580 and 890 cm^{-1}, with another weaker band at 770 cm^{-1}. The 580 an 770 cm^{-1} bands are very sensitive to surface condition, with both the absolute and relative intensities changing with successive cycles of O_2 exposure and Ar^+-ion bombardment. Erskine and co-workers [24] have reported EELS data for O_2 chemisorption on ordered Al (111) surfaces showing a 640 cm^{-1} surface Al-O mode and an 840 cm^{-1} subsurface Al-O vibration, of approximately equal intensity, together with a weak 320 cm^{-1} peak also arising from subsurface O. Brüesch et al. [25] have performed multiple-reflection IRRAS on very thin films (down to 5 Å) of Al_2O_3 sputter-deposited on Au and Si as well as on natural-oxide films (down to 15 Å) on Al. The dominant feature is a mode the frequency of which is strongly dependent on Al_2O_3 film thickness below 20 Å. At sub-monolayer coverage, this is the 840 cm^{-1} subsurface Al-O vibration [24] which shifts to 950 cm^{-1} for a 20 Å film and develops into the bulk Al_2O_3 LO phonon at greater thicknesses. The results of these two studies indicate that the O/Al vibrational spectrum is very structure-sensitive. For the present disordered, Ar^+-implanted Al substrate, the appearance of a band at 880 cm^{-1} (corresponding [25] to about 3 Å of Al_2O_3) indicates that O does not occupy well-defined subsurface sites, as for the ordered Al (111) surface, but instead forms the beginning of an Al_2O_3-like structure. The width of this band, about 100 cm^{-1}, is larger than the IRRAS resolution and agrees with that reported by Bruesch et al. [25]. The 580 and 770 cm^{-1} modes (Fig. 5) might then correspond to perturbed surface and subsurface Al-O vibrations, analogous to those observed in EELS [24]. A detailed interpretation requires data for more well-characterized surfaces.

Given the observed noise level, equivalent to an adsorption-induced change in $\delta r_p/r_p$ of about 0.05%, and signal/noise ratio (about 20:1 in Fig.

4), we estimate the minimum detectable coverage of oxygen on aluminum to be approximately 0.1 monolayers. This compares favorably with results for other polarization-modulation experiments at much shorter wavelengths using a blackbody source. Leonard et al. [15], using a rotating polarizer apparatus with phase-shift measurement, report a long-term stability in ψ of 0.01° for a metallic substrate, which corresponds to an adsorption-induced change in $(I_s - I_p)/(I_s + I_p)$ of 0.04%. Using a similar approach, Mahaffy and Dignam [27] obtained a noise level equivalent to about 0.05% for a single reflection from a nickel surface. Golden et al. [19], using a PEM, report noise levels of about 0.01%, and rotating polarizer experiments in which lock-in amplification has been successful [9,16,28] report similarly low noise levels.

The energy scale in Figs. 4 and 5 was obtained by measuring transmission spectra of standard organic compounds. The resolution, about 40 cm^{-1}, is comparable to the best routinely attainable in EELS. As discussed above, the present experiments did not use a monochromator. Tuning was performed by varying the diode temperature, resulting in a narrow (~40 cm^{-1}) band of several overlapping modes the center of which gradually swept through the range of the diode. Since these experiments are not intensity-limited, use of a monochromator (driven in step with the laser temperature) should afford a resolution of a few cm^{-1} or better.

One final point concerns the asymmetry of the IRRAS bands (particularly evident in Fig. 4) and the difference in the sign of $\delta r_p/r_p$ at the peak and in the "wings". Both effects can be understood using the arguments developed by Greenler [29] and the expressions derived by McIntyre and Aspnes [30] for $\delta r_p^2/r_p^2$ and $\delta r_s^2/r_s^2$ in the thin-film limit. The IRRAS signal in the "wings" depends mainly on the real index of the adsorbate layer, and the "anomalous dispersion" of this quantity results in the asymmetry. An increase in the

magnitude of the real index (for the present set of experimental conditions) results in a positive $\delta r_p/r_p$; whereas, an increase in the imaginary index causes a negative change. This accounts for the variation in sign of $\delta r_p/r_p$ across the absorption band.

SUMMARY

This communication reports the feasibility of using tunable lead salt diode lasers as spectrally bright light sources for Infrared Reflection Absorption Spectrosocpy (IRRAS) of surface chemical species from 400 to 1700 cm^{-1}, well beyond the range of conventional blackbody sources. Submonolayer sensitivity was demonstrated for Al-O modes on disordered polycrystalline Al at 580, 770 and 890 cm^{-1}. Comparison with EELS results for O_2 on ordered Al (111) indicates the sensitivity of the vibrational spectrum to the substrate surface structure.

Future development of the apparatus will focus on improvements in resolution and in signal-to-noise-ratio. The most obvious requirement is for the addition of a monochromator to supplement the present crude method of scanning by diode temperature variation alone. Refinements in the electronics (principally in the VCA and in the boxcar gating) are expected to reduce the noise level. The IRRAS system will also be combined with a more fully instrumented UHV chamber to allow experiments on better characterized surfaces. For those investigations not requiring very low photon energies, modulation by means of a ZnSe PEM, instead of the rotating polarizer, should yield a further reduction in the noise level.

Diode-laser polarization-modulation IRRAS is sensitive and non-intrusive and discriminates against ambient absorption. Thus it constitutes a useful new technique for surface studies.

ACKNOWLEDGEMENTS

We are grateful to Andy Baronavski, Orest Glembocki, Ron Holm and Ed Palik for the loan of various pieces of equipment.

REFERENCES

1. "Electron Energy Loss Spectroscopy and Surface Vibrations", Ed. H. Ibach and D.L. Mills (Academic, New York, 1982).

2. "Third International Conference on Vibrations at Surfaces", Ed. C.R. Brundle and H. Morawitz; J. Electron Spectrosc. Relat. Phenom. 29, 30 (1983).

3. C.G. Pantano and T.E. Madey, Applic. Surf. Sci. 7, 115 (1981).

4. P. Pianetta, I. Lindau, P.E. Gregory, C.M. Garner and W.E. Spicer, Surf. Sci. 72, 298 (1978).

5. R. Ryberg, J. Phys. (Paris) Colloq. 44, C10-421 (1983).

6. G.T. Haller, Catal. Rev. - Sci. Eng. 23, 447 (1981).

7. M.J. Dignam and J. Fedyk, Appl. Spectrosc. Rev. 14, 249 (1978); J.D. Fedyk, P. Mahaffy and M.J. Dignam, Surf. Sci. 89, 404 (1979).

8. S. Chiang, R.G. Tobin and P.L. Richards, J. Vac. Sci. Technol. A 2, 1069 (1984).

9. F.M. Hoffmann, Surf. Sci. Reports 3, 107 (1983).

10. D.K. Lambert, J. Electron Spectrosc. Relat. Phenom. 30, 59 (1983); Phys. Rev. Letters 50, 2106 (1983).

11. R. Ryberg, Phys. Rev. B 31, 2545 (1985); J. Chem. Phys. 82, 567 (1985).

12. R.K. Kim and R. Braunstein, Appl. Opt. 23, 1166 (1984).

13. J.C. Campuzano and R.G. Greenler, Rev. Sci. Instrum. 52, 678 (1981).

14. R.W. Stobie, B. Rao and M.J. Dignam, Appl. Opt. 14, 999 (1975); J. Opt. Soc. Am. 63, 25 (1975).

15. T.A. Leonard, J. Loomis, K.G. Harding and M. Scott, Opt. Engineer. 21, 971 (1982); T.A. Leonard, J. Stubbs and J.S. Loomis in "Optical Thin Films", S.P.I.E. Vol 325, 149 (1982).

16. A.M. Bradshaw, Applic. Surf. Sci. 11/12, 712 (1982).

17. T. Wadayama, T. Saito and W. Suetaka, Applic. Surf. Sci. 20, 199 (1984); T. Wadayama, K. Monma and W. Suetaka, J. Phys. Chem. 87, 3181 (1983).

18. M.E. Pedinoff, M. Braunstein and O.M. Stafsudd, Appl. Opt. 16, 2849 (1977).

19. W.G. Golden, D.S. Dunn and J. Overend, J. Catal. 71, 395 (1981); W.G. Golden, D.D. Saperstein, M.W. Severson and J. Overend, J. Phys. Chem. 88, 574 (1984).

20. T.A. Leonard in "Los Alamos Conference on Optics", S.P.I.E. Vo. 288, 129 (1981).

21. J.C. Cheng, L.A. Nafie, S.D. Allen and A.I. Braunstein, Appl. Opt. 15, 1960 (1976).

22. I. Chabay and G. Holzwarth, Appl. Opt. 14, 454 (1975).

23. R.M.A. Azzam and N.M. Bashara, "Ellipsometry and Polarized Light", (North Holland, Amsterdam, 1978).

24. J.L. Erskine and R.L. Strong, Phys. Rev. B 25, 5547 (1982); R.L. Strong, B. Firey, F.W. de Wette and J.L. Erskine, Phys. Rev. B 26, 3483 (1982).

25. P. Brüesch, R. Kötz, H. Neff and L. Pietronero, Phys. Rev. B 29, 4691 (1984).

26. P. Hofmann, W. Wyrobisch and A.M. Bradshaw, Surf. Sci. 80, 344 (1979); B.E. Hayden, W. Wyrobisch, W. Oppermann, S. Hachicha, P. Hofmann and A.M. Bradshaw, Surf. Sci. 109, 207 (1981).

27. P.R. Mahaffy and M.J. Dignam, Surf. Sci. 97, 377 (1980).

28. H. Pfnür, D. Menzel, F.M. Hoffmann, A. Ortega and A.M. Bradshaw, Surf. Sci. 93, 431 (1980).

29. R.G. Greenler, J. Chem. Phys. 44, 310 (1966); 50, 1963 (1969).

30. J.D.E. McIntyre and D.E. Aspnes, Surf. Sci. 24, 417 (1971).

FIGURE CAPTIONS

1. Schematic of the optical and electronic system. Various focusing and beam-steering mirrors are not shown. Inset shows the signal waveform (schematic) before and after the lock-in and the gating sequence (see text). For clarity, the rotation frequency (125 Hz) has been greatly exaggerated, relative to the chopper frequency (5 kHz), and the b/a ratio in waveform "B" is also greatly magnified.

2. Plot of multi-mode power, vs. photon energy (cm^{-1}), at 90% of maximum current for several different diodes.

3. Representative mode patterns for the same diodes as in Fig. 2. For each diode, the operating tempeature, T, current, I, and power, P, are indicated.

4. IRRAS results for dissociative chemisorption of O_2 on Al in the region of the sub-surface Al-O vibration (ref. 24). The data were obtained by subtractng the average of two scans for the clean surface from the average of two scans after a 300 Langmuir exposure. The resolution is estimated to be 40 cm^{-1}. Absorption increases in the direction of negative $\delta r_p/r_p$. Data were obtained using the rotating polarizer method.

5. Same as Fig. 4 but for the lower-energy Al-O modes.

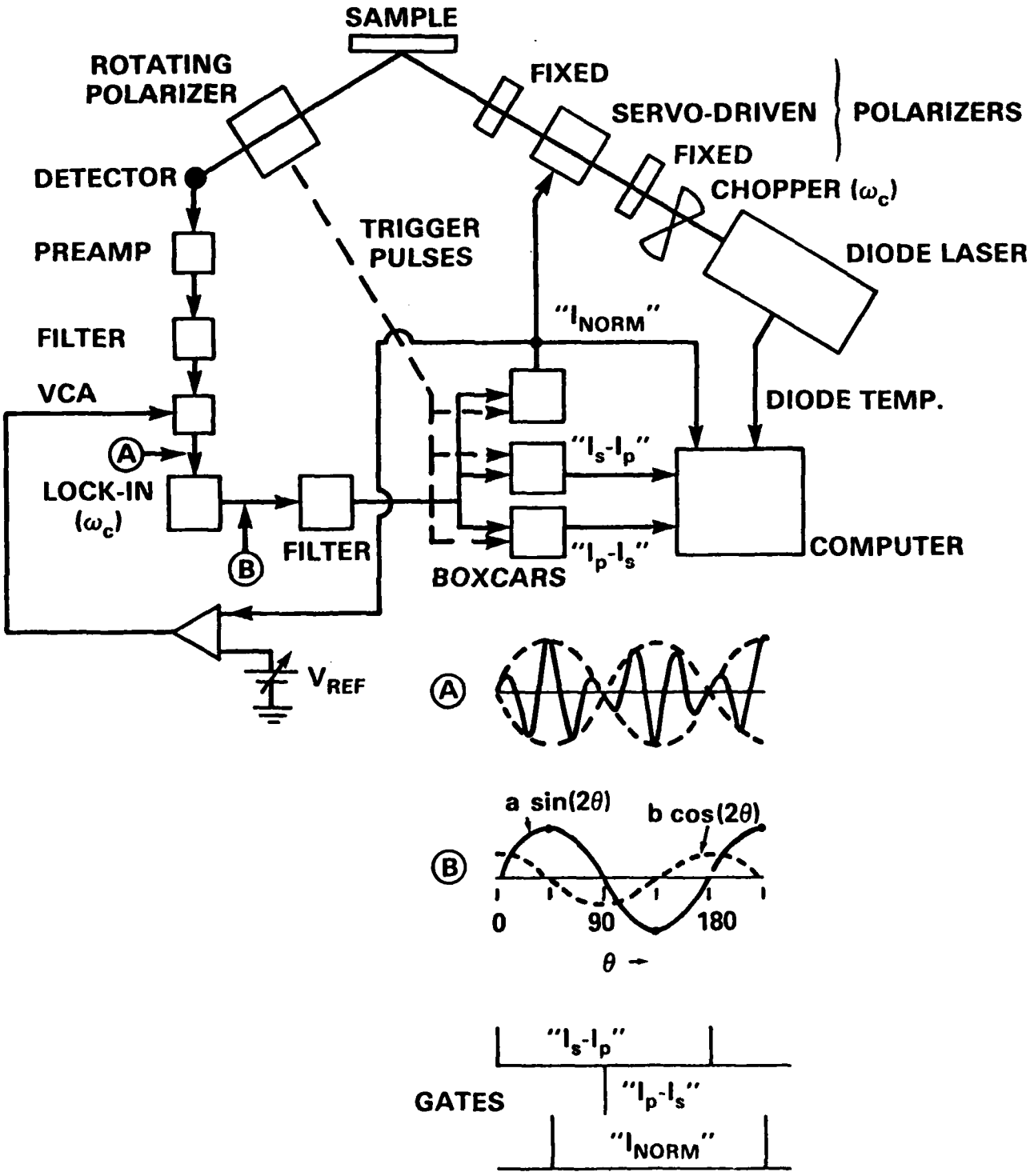
SAMPLE
ROTATING POLARIZER
FIXED
SERVO-DRIVEN
POLARIZERS
FIXED
DETECTOR
CHOPPER (ω_c)
TRIGGER PULSES
PREAMP
DIODE LASER
FILTER
"I_{NORM}"
VCA
DIODE TEMP.
A
"I_s-I_p"
LOCK-IN (ω_c)
FILTER
COMPUTER
B
"I_p-I_s"
BOXCARS
V_{REF}
A
a sin(2θ)
b cos(2θ)
B
0
90
180
θ →
"I_s-I_p"
GATES
"I_p-I_s"
"I_{NORM}"

Fig. 1

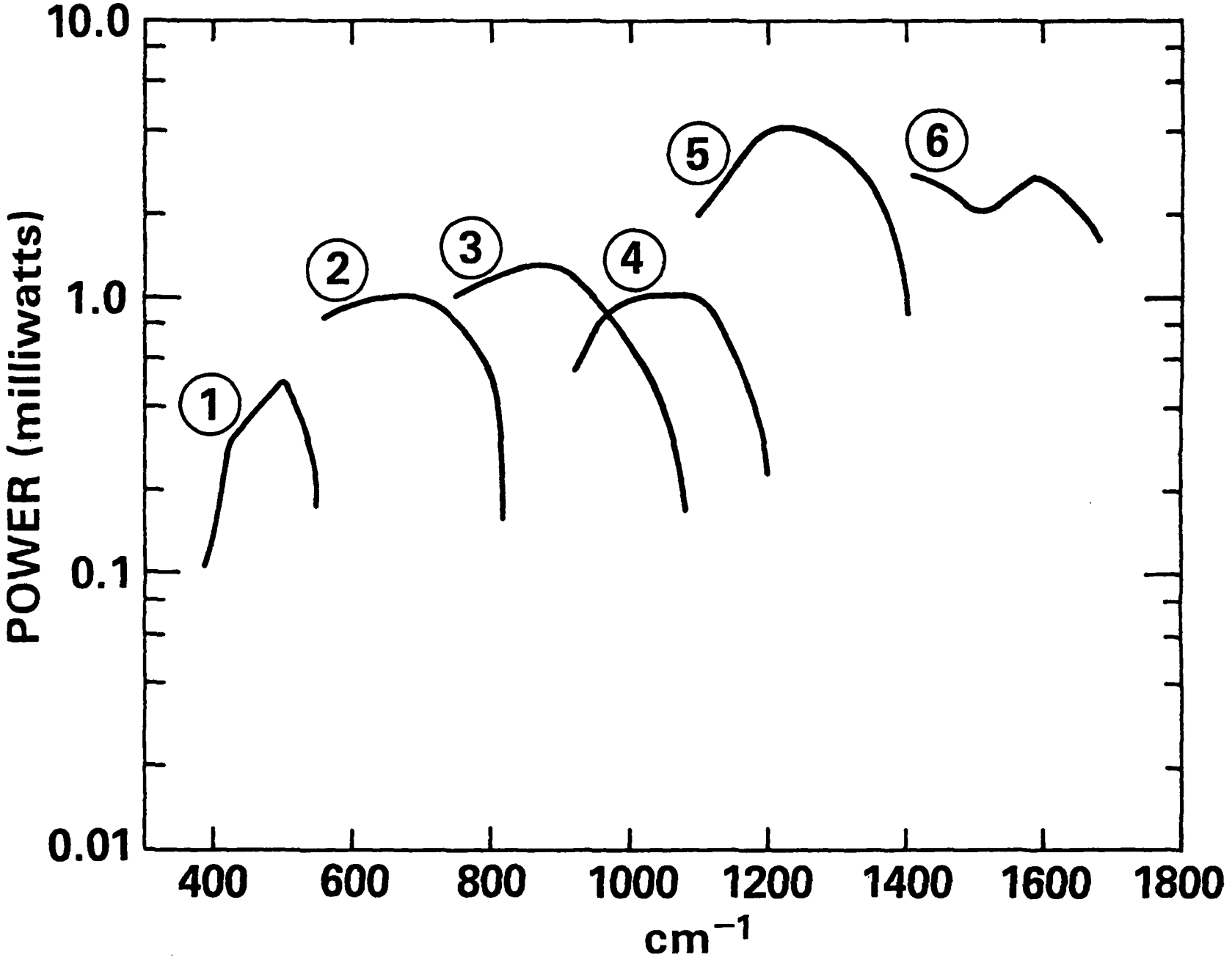
10.0
1.0
0.1
0.01
POWER (milliwatts)
400
600
800
1000
1200
1400
1600
1800
cm⁻¹
1
2
3
4
5
6

LI

Fig 2

DIODE NUMBER

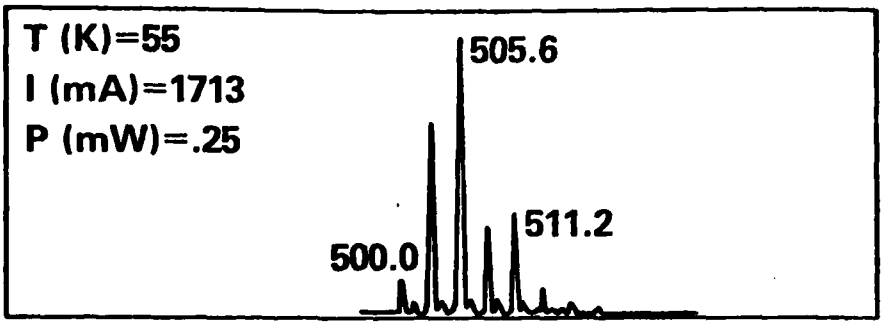

①

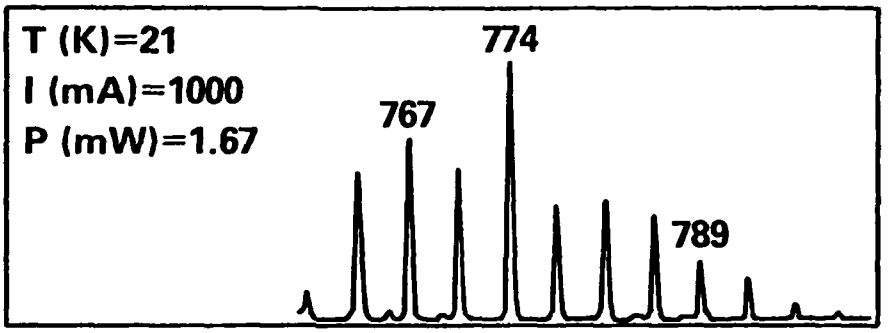

②

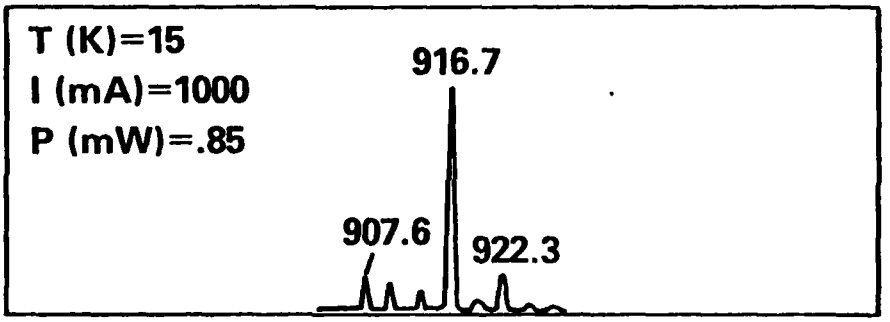

③

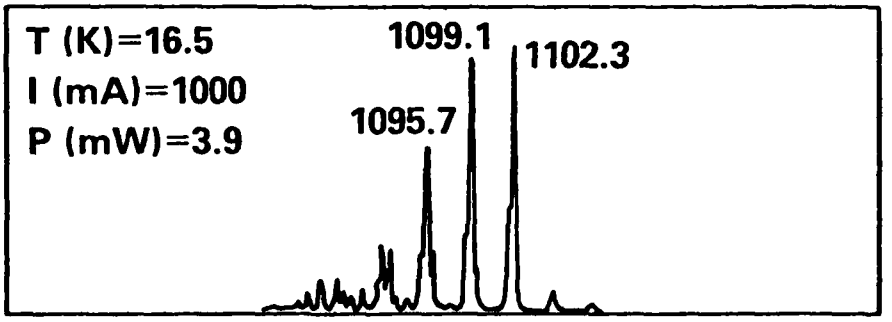

④

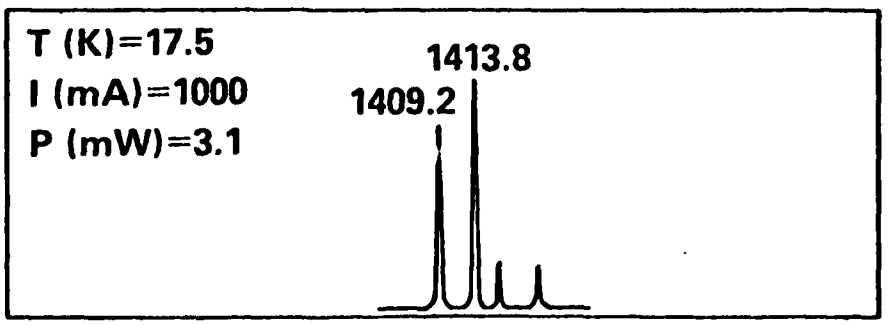

⑥

Fig. 3

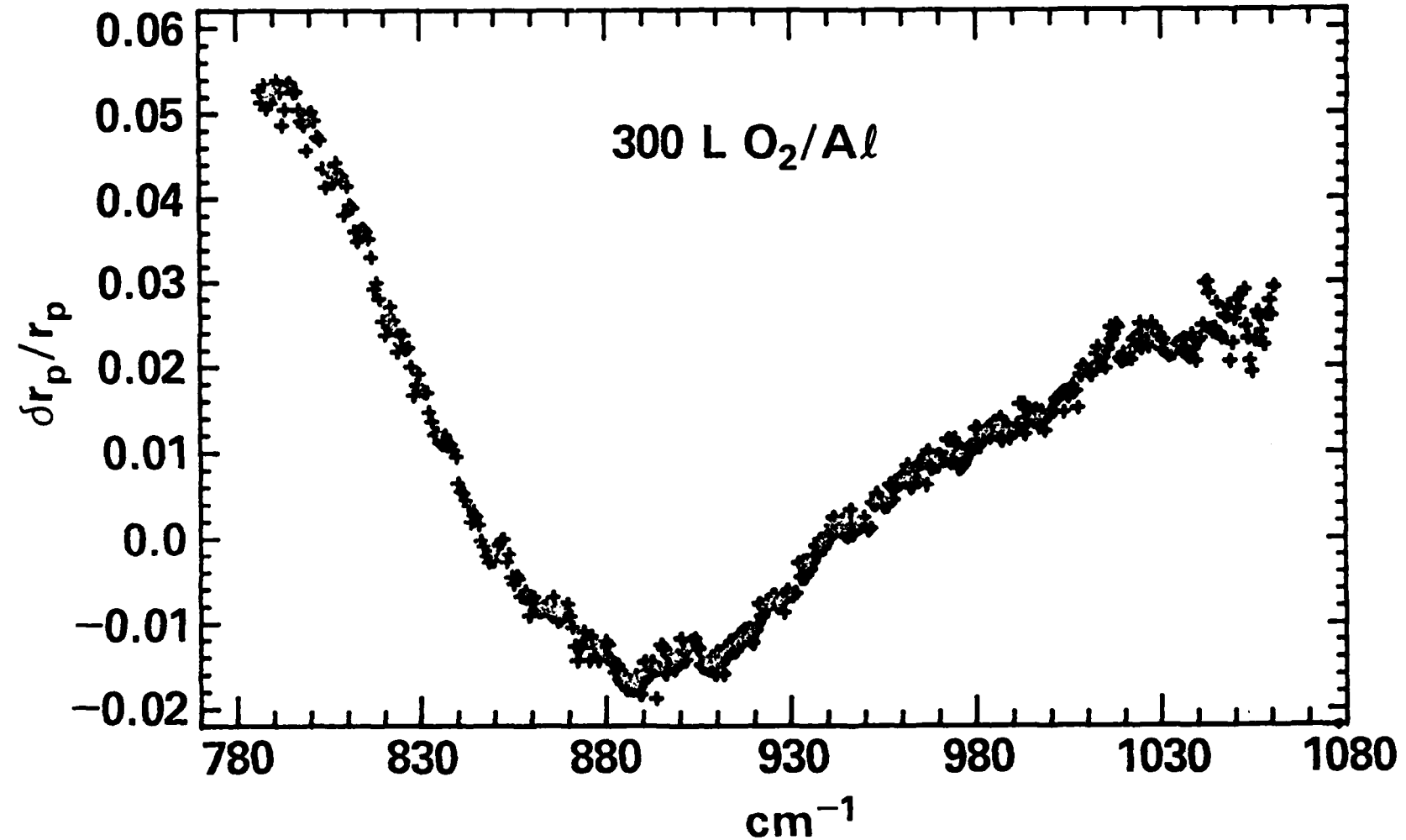
300 L O_2/Aℓ
$\delta r_p/r_p$
0.06
0.05
0.04
0.03
0.02
0.01
0.0
−0.01
−0.02
780
830
880
930
980
1030
1080
cm^{-1}

Fig 4

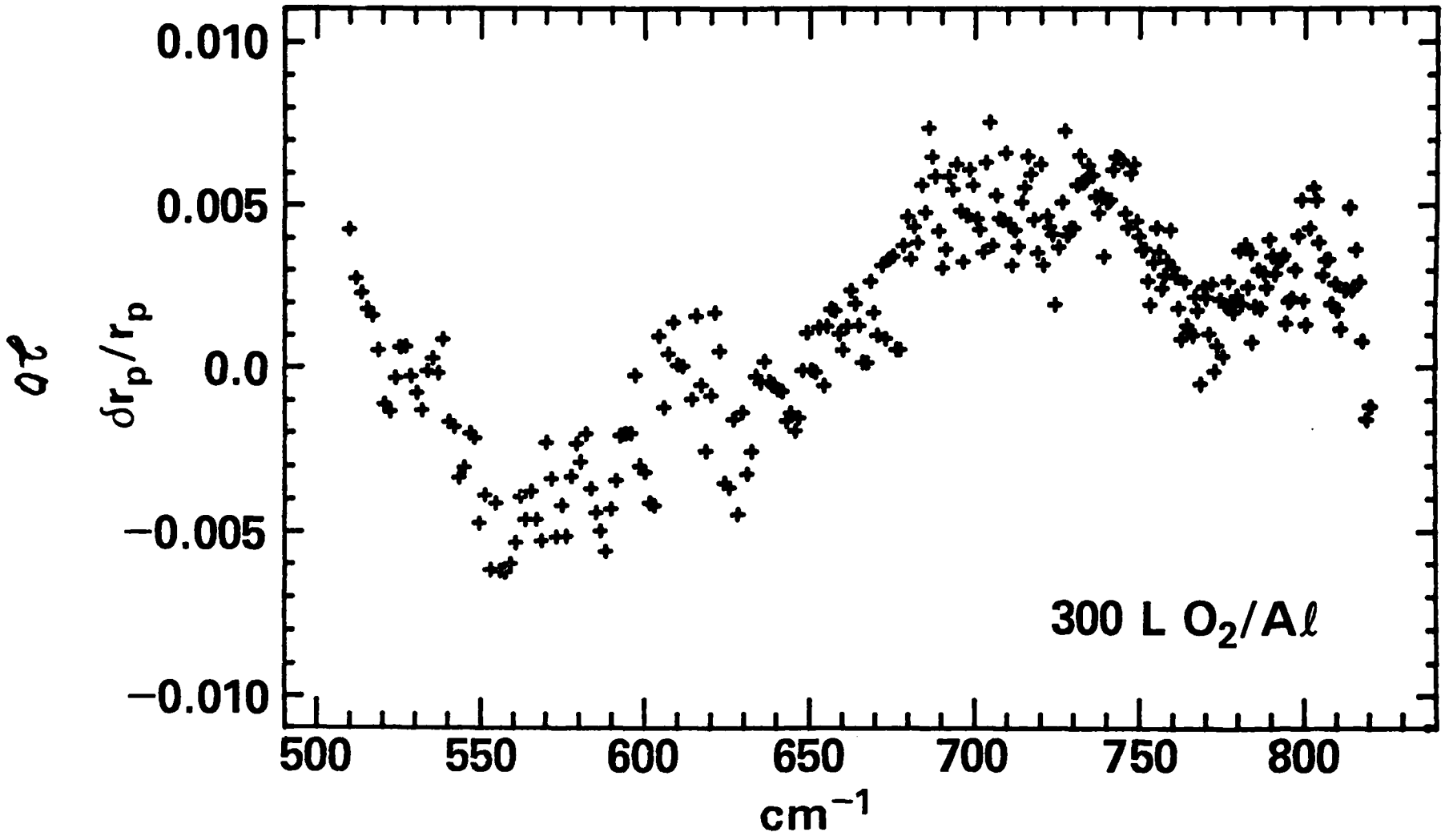
0.010
0.005
0.0
−0.005
−0.010
$\delta r_p/r_p$
500
550
600
650
700
750
800
cm^{-1}
300 L O_2/Aℓ

Fig 5

END

FILMED

11-85

DTIC